

A STATISTICAL THERMODYNAMICS MODEL OF SLAGS:
APPLICATIONS TO SYSTEMS CONTAINING S, F, P₂O₅ AND Cr OXIDES

H. Gaye*, J. Lehmann*, T. Matsumiya**, W. Yamada**

* IRSID, Maizières-lès-Metz, France

** NSC, Advanced Materials and Technology Labs, Kawasaki, Japan

Synopsis: New developments, made through a cooperative research between Nippon Steel Corp. and IRSID, of IRSID's slag model are presented.

Two main extensions of the model formalism have been made.

The first one consists in an extension of the formalism to polyanionic slags. Applications of this extension to sulphur and fluorine bearing slags are proposed.

The aim of the second extension is the description of the singular behaviour of some oxides, as P₂O₅ or Al₂O₃. An application to high and low P₂O₅ slags is shown.

More "classical" extensions to Cr₂O₃ bearing systems are also presented.

Key words: slag model, activities, sulphur, fluorine, phosphorus, chromium, titanium.

1. Introduction.

The basis of the slag model developed at IRSID was presented at the 2nd International Symposium on Metallurgical Slags and Fluxes [1]. At that stage, the model gave a fairly good description of the phase diagrams and component activities for the SiO₂-Al₂O₃-Fe₂O₃-FeO-MnO-MgO-CaO system. Efforts have then been devoted to inserting this model in specific procedures for the direct calculation of phase diagrams (crystallization paths), and for the study of iron- and steelmaking reactions: slag-metal-gas reactions, precipitation of inclusions in steel, ... [2]. In order to extend its validity domain, a cooperative study between NSC and IRSID was decided. The results of this cooperation are presented here. A part of this work required an extension of the model formalism in order to take into account slags containing other anions than oxygen: sulphur and fluorine and also in order to represent the singular behaviour of some oxides, such as P₂O₅ (and Al₂O₃ in the future). Another part of this study consisted in extending the covered range to Cr₂O₃ bearing slags.

2. Basis of the model.

For the polyanionic formalism, the description of slag structure remains basically the same as for pure oxides. Two sublattices are considered:

- an anionic sublattice filled with the divalent anions, here oxygen, sulphur and difluorine anions,
- a cationic sublattice. On this sublattice, are distributed the cations, but also "cationic entities", constituted by cations doubly linked to one oxygen. This extension has been made in order to represent the behaviour of some oxides, which do not release all their oxygens to the anionic sublattice. As it will be seen later, such a representation is used for P₂O₅: two phosphorus "cationic entities" P⁵⁺ and (PO)³⁺ are assumed, which are distributed on the cationic sublattice. The existence of the latter entity is not surprising because in the (PO₄³⁻) tetrahedron, one oxygen is doubly linked to

phosphorus. It is believed, that the same approach can be used to represent the amphoteric behaviour of Al_2O_3 , for which the present description is not entirely satisfactory in the silica rich part of the $SiO_2-Al_2O_3$ binary (mullite field of complex slags).

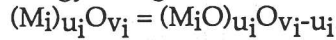
The cationic sublattice is filled with the different cations and cationic species in decreasing order of their charges. The structure is then described in terms of cells, which contain a central anion and two cations (or cationic entities). Starting from this microscopic description, the expression of the degeneracy of the system is written, using the quasi-chemical approach. The total energy is then written with three types of parameters. These parameters are all binary parameters and they have so far been assumed to be temperature independent.

2.1. Parameters of the model.

Cells Formation: in the polyanionic model, two types of cell formation parameter are used:
 - W_{ij}^A , associated, for each anion, to the formation of asymmetric cells: $1/2 (i-A-i) + 1/2 (j-A-j) = (i-A-j)$
 - W_{i1}^{OA} , representing the stability of the A-symmetric cell relative to the oxygen symmetric cell:
 $(i-O-i) + A = (i-A-i) + O$

The most convenient reference states will be chosen for the various anions. For the oxysulphides, we have selected, for oxygen and sulphur, the 1% solution in liquid iron.

Cationic entities formation: these parameters, noted δg_i , are specific to oxides which can give two cationic entities. They represent the energy change associated to the following reaction:



Interactions between cells: in the liquid oxide model, only one independent cell interaction parameter is used per binary system, that is E_{ij}^O , representing the interaction between the cells (i-O-i) and (i-O-j), i having a higher valency than j. All the interactions have been expressed with this single parameter, by using the following additive rule:

$$E(i-O-i)-(j-O-k) = E(i-O-i)-(i-O-j) + E(i-O-i)-(i-O-k) = E_{ij}^O + E_{ik}^O$$

In order to consider only binary interaction parameters for the polyanionic systems, this additive rule has been extended in the following way:

$$E(i-A-i)-(j-B-k) = E(i-A-i)-(i-B-j) + E(i-A-i)-(i-B-k) \\ = E(i-A-i)-(i-A-j) + E(i-A-i)-(i-B-i) + E(i-A-i)-(i-A-k) + E(i-A-i)-(i-B-i) = E_{ij}^A + E_{ik}^B + 2E_{i1}^{AB}$$

Thus, in the polyanionic model, the interaction parameters are E_{ij}^A , representing interaction

<p>Free Energy:</p> $G = \sum_i \delta g_i \cdot X_{iO} + \sum_{i,i,k} W_{ij}^k R_{ij}^k + 2RT \sum_{i,k} R_{ii}^k \ln Q_{ik}$ $- RT \left(\sum_{i=1}^{m-1} a_i \left(D_i \ln \frac{D_i}{V_i} - D_{i+1} \ln \frac{D_{i+1}}{V_i} \right) + 2 \sum_{i=1}^m V_i \ln \frac{V_i}{D_1} - \sum_{i,j,k} R_{ij}^k \ln \frac{R_{ij}^k}{D_1} \right)$ <p>Mass balance equations:</p> <p>cations: $\sum_{j,k} R_{ij}^k = V_i$ anions: $\sum_{i,j} R_{ij}^k = V^k$</p> <p>Maximization of the partition function:</p> $R_{ii}^1 \cdot R_{jj}^1 = (R_{ij}^1 / P_{ij}^1)^2 \quad i,j=1 \dots m$ $R_{ii}^1 \cdot R_{11}^k / R_{11}^1 = R_{ii}^k / P_{ii}^k \quad i=1 \dots m, k=2 \dots p$ $R_{ii}^1 \cdot R_{jj}^1 \cdot (R_{11}^k)^2 = (R_{11}^1)^2 \cdot (R_{ij}^k / P_{ij}^k)^2 \quad i,j=1 \dots m, k=2 \dots p$	<p>Notations:</p> <p>u_{ik} (i=1...m; k=1...p)</p> <p>v_{ik} (i=1...m; k=1...p)</p> <p>$a_i = u_{ik} / v_{ik}$</p> <p>stoichiometric coefficients of $(M_i)_{u_{ik}} (A_k)_{v_{ik}}$</p> <p>$X_{ik}$: mole numbers of $(M_i)_{u_{ik}} (A_k)_{v_{ik}}$</p> <p>$R_{ij}^k$: number of cells i-k-j</p> <p>$V_i = \sum_k v_{ik} X_{ik}$ $V^k = \sum_i v_{ik} X_{ik}$</p> <p>$D_i = \sum_{j=i}^m V_j$</p>
<p>Table 1: Expression of the free energy</p>	$RT \ln Q_{ik} = \frac{1}{D_1} \left(\sum_j V_j E_{ij}^k + \sum_l V_l E_i^{kl} \right)$ $RT \ln P_{ij}^k = W_{11}^k - (1 - \delta_{ij}) (W_{ii}^k + W_{jj}^k) - W_{ij}^k + RT \ln (Q_{i1} \cdot Q_{j1} \cdot \left(\frac{Q_{1k}}{Q_{11}} \right)^2) - 2\delta_{ij} RT \ln Q_{ik}$

between (i-A-i) and (i-A-j) and E_i^{AB} , representing interaction between (i-A-i) and (i-B-i).

Up to now, this additivity assumption, which allows the transformation of all high-order interactions to binary interactions, did not prevent from obtaining a satisfactory description of the properties of the systems studied. But, in the future, if it is proved to be necessary for some specific systems, this assumption could eventually be released.

For some systems, a linear dependence as a function of composition has been adopted for the formation and interaction parameters.

Table 1 gives the expression of the Gibbs free energy of the system. This formula holds for any number of cations and of divalent anions. In this expression, the mole numbers of cells and cationic entities must be calculated by the condition of maximisation of the partition function under the mass balance constraints. The number of resulting equations increases very fast with the number of slag components. Thus, for m cations and p anions, the system contains $pm(m+1)/2-(m-2)(p-1)$ equations. Such a large number of equations would lead to prohibitive computing times. Fortunately, using a change of variables, it is possible to reduce the size of the system to a number of equations which varies linearly with the number of components ($(m+p-1)$ equations for m cations and p anions).

2.2. Assessment of the model parameters.

Although all the model parameters are binary parameters, it is often necessary to assess them on systems containing more than two components. This can be due to several factors: either the binary data is lacking or is not accurate enough, or the liquid domain is too limited. In order to handle these multicomponent data, a specific computer code based on a least squares method has been developed. It can treat together data of various origins: component activities, slag/metal/gas equilibrium distribution ratios, chemical potentials of stoichiometric compounds, phase diagrams and is very efficient when a large number of experimental data points are available.

A complete list of the parameters that have so far been assessed is given in Table 2.

3. Sulphur- and Fluor- bearing systems.

The various coefficients of the model specific to the oxisulphide systems have been assessed using most of the experimental data on sulphide capacity available in the literature. The experiments consist of gas-slag, and, for iron oxide-bearing slags, of metal-slag equilibria. Some experiments on sulphur solubility are also available. Up to now, we have restricted our investigations to the system: $\text{SiO}_2\text{-Al}_2\text{O}_3\text{-Cr}_2\text{O}_3\text{-Fe}_2\text{O}_3\text{-CrO-FeO-MnO-MgO-CaO}$, for which the oxide model was completely assessed. For the sulphide cells, it was only necessary to assess the formation energy of asymmetric cells, without any composition dependence. No interaction energy parameters are required, because of the limited range of sulphur solubility in metallurgical slags. The behaviour of sulphur is very sensitive to the parameters representing the relative stability between oxides and sulphides for the various cations (right hand side of Table 2).

The validity of the assessment is illustrated in figure 1a, which compares the decimal logarithms of the measured and calculated sulphide capacities for more than 600 experimental points. The standard deviation between experimental and calculated values correspond to a relative error on the sulphide capacity of about 30%, which is in the same range as experimental uncertainties. In comparison, the sulphide capacities for the same set of data have been calculated with Sosinski and Sommerville's model [3], based on a correlation in terms of Optical Basicity and compared to the experimental values (figure 1b). If this correlation is rather satisfactory for the system $\text{SiO}_2\text{-Al}_2\text{O}_3\text{-CaO-MgO}$ (right hand side of the experimental points), it can lead to errors up to two or three orders of magnitude for FeO and MnO bearing slags (left hand side of the experimental points). Note that this correlation leads to a large overestimation of the desulphurizing power of MnO, materialized by the wrong slope of points for MnO-containing compositions.

For fluorine bearing slags, the assessment of parameters was made mostly on phase diagram information (ternary systems based on CaO-CaF_2 , with SiO_2 , Al_2O_3 , FeO, MnO and MgO) and component activities (systems $\text{SiO}_2\text{-CaO-CaF}_2$ and MnO-CaO-CaF_2). In all these systems, the model indicates that most of the fluorine anions would be associated with calcium cations. The agreement with experimental data is in general satisfactory, except in the ternary MgO-CaO-CaF_2 .

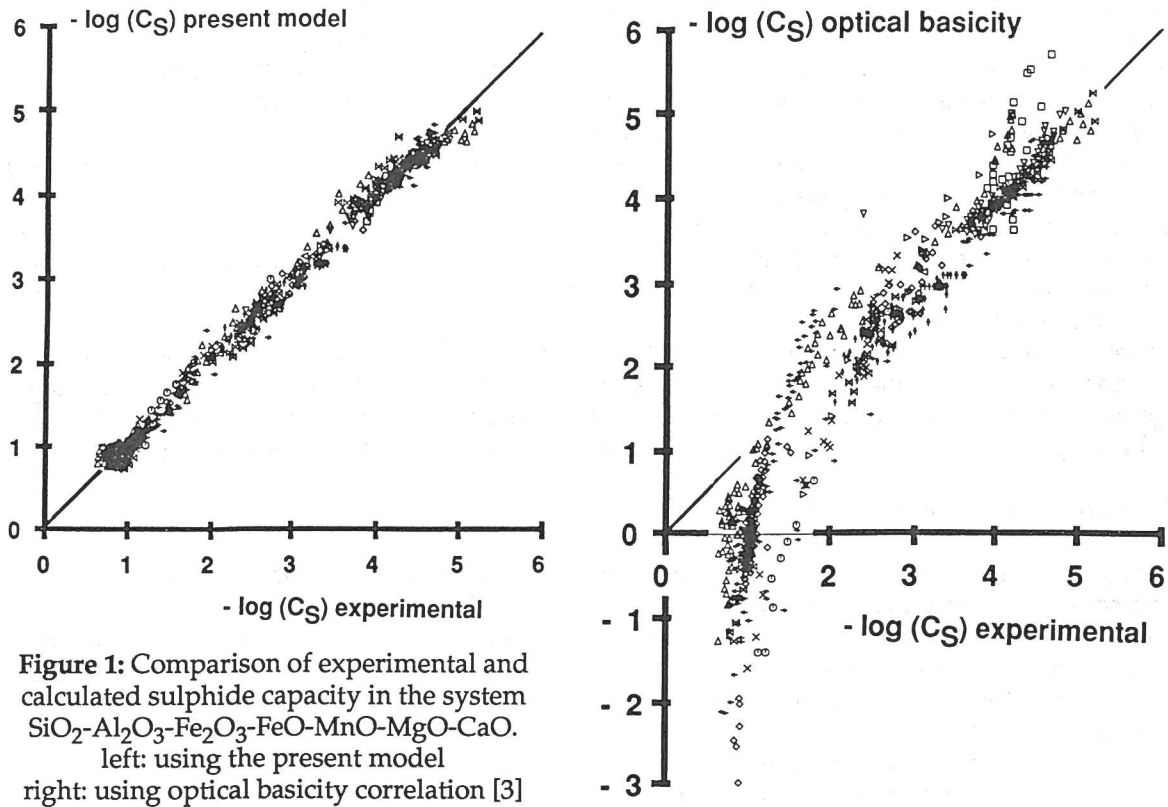


Figure 1: Comparison of experimental and calculated sulphide capacity in the system $\text{SiO}_2\text{-Al}_2\text{O}_3\text{-Fe}_2\text{O}_3\text{-FeO-MnO-MgO-CaO}$.
 left: using the present model
 right: using optical basicity correlation [3]

4. P₂O₅- bearing slags.

Since the previous assessment of these systems [4], a large improvement has been obtained by considering the two cationic entities P⁵⁺ and (PO)³⁺. The parameters listed in Table 2 have been obtained mostly from phosphorus and oxygen distribution coefficients between slag and metal in the

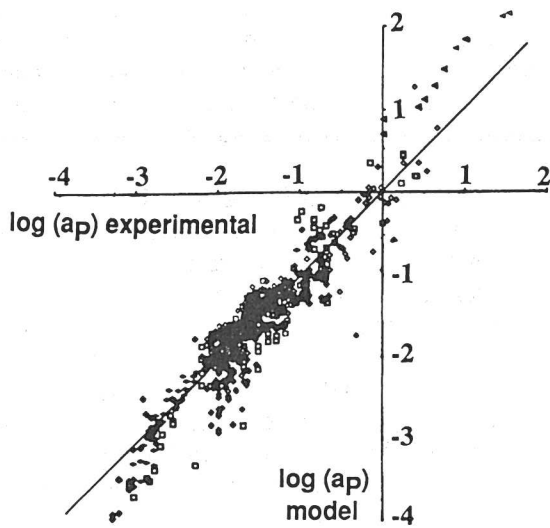


Figure 2: Comparison between calculated and experimental values of phosphorus activity. System: $\text{SiO}_2\text{-P}_2\text{O}_5\text{-Al}_2\text{O}_3\text{-Fe}_2\text{O}_3\text{-FeO-MnO-CaO}$ with %P₂O₅ ≤ 40 and %FeO_t ≤ 70.

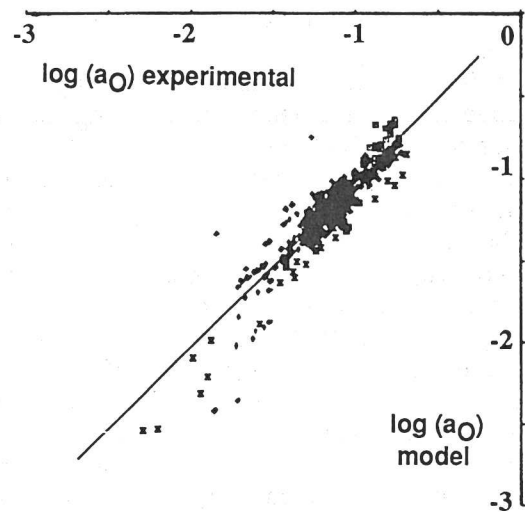


Figure 3: Comparison between calculated and experimental values of oxygen activity. Same system as Figure 2.

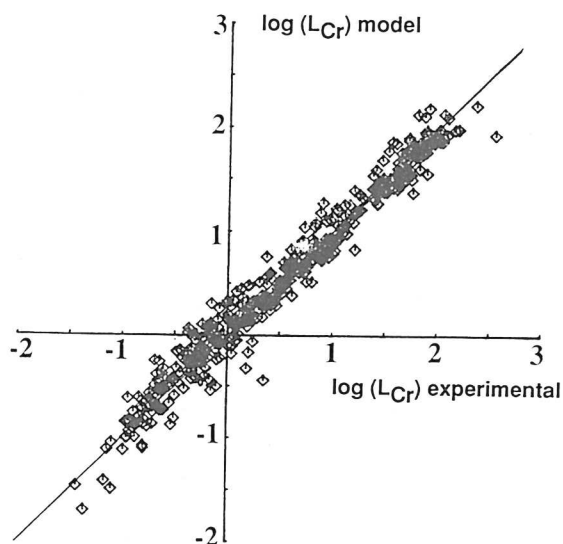


Figure 4: Comparison between calculated and experimental values of Cr slag-metal equilibrium distribution ratio: $L_{Cr} = (\%Cr_2O_3)_t / a_{Cr}$. System: $SiO_2-Al_2O_3-Cr_2O_3-Fe_2O_3-CrO-FeO-MnO-MgO-CaO$

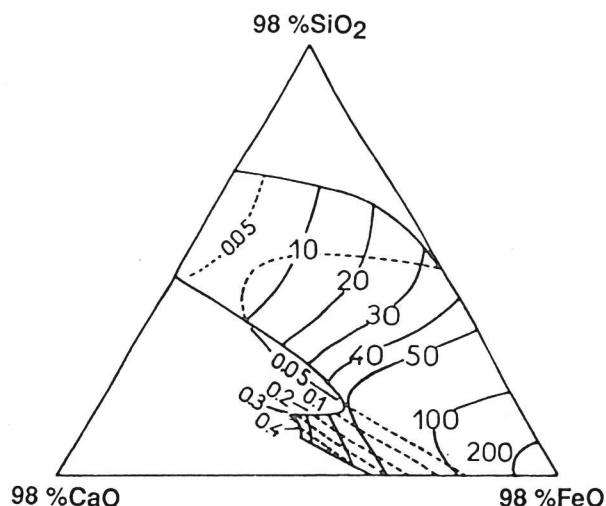


Figure 5: Computed values of iso Cr distribution ratio L_{Cr} (solid lines) and iso ratio $Cr^{3+}/(Cr^{3+}+Cr^{2+})$ (dotted lines) in the system $SiO_2-FeO^*-CaO-2\%Cr_2O_3$ in equilibrium with iron at $1600^\circ C$.

$SiO_2-P_2O_5-Al_2O_3-Fe_2O_3-FeO-MnO-CaO$ system with $\%P_2O_5 \leq 40$ and $\%FeO_t \leq 70$, using a population of more than 700 data points published in the literature, which correspond to typical high and low P refining slags, as well as special dephosphorizing slags with very low P_2O_5 contents.

As shown in Figures 2 and 3, the general agreement between model predictions and experimental values is rather good. In this evaluation, the model provides both the oxygen activity (from the Fe-FeO equilibrium for the computed Fe^{3+}/Fe^{2+} distribution) and the phosphorus activity (from the computed P_2O_5 and oxygen activities). The net result on phosphorus estimation thus combines the uncertainties on all these quantities. The precision of the prediction is of the same order of magnitude as the experimental scatter, which can reach 200 or 300%. The only systematic deviation concerns a set of data points at very low phosphorus activity (below 0.001%) for which the model seems to underestimate its value. These slags correspond to SiO_2-FeO^*-CaO and $Al_2O_3-FeO^*-CaO$ domains with $\%P_2O_5 < 0.5$.

5. Cr_2O_3 bearing systems.

The assessment of slags containing chromium oxides was made by considering the coexistence of both Cr^{3+} and Cr^{2+} . The parameters pertaining to Cr^{3+} were mostly deduced from data on phase diagrams in oxidizing conditions [4], whereas those pertaining to Cr^{2+} were mostly deduced from data on Cr partition between metal and $SiO_2-Al_2O_3-Cr_2O_3-Fe_2O_3-CrO-FeO-MnO-MgO-CaO$ slags.

As shown on Figure 4, the evaluation of the Cr partition coefficient is quite precise. For systems in equilibrium with metallic iron (Figure 5), the model predicts that the Cr^{3+}/Cr^{2+} ratio follows the same trend as the Fe^{3+}/Fe^{2+} ratio: it is at its maximum near CaO saturation and decreases markedly for SiO_2 rich slags.

6. Conclusions.

The transformation of the oxide slag model into a polyanionic model respects the features which make the versatility of the original model: use of binary parameters only, possibility of use for multicomponent systems, and it provides a quite accurate estimation of the thermodynamic properties of complex iron- and steelmaking slags. The software which has been developed around it to analyse and control metallurgical reactions, in particular ladle metallurgy and inclusions control, is presently in use as a routine tool in most French steelplants.

Cations i - j	O Cells		S Cells	F Cells
	W _{ij}	E _{ij}	W _{ij}	W _{ij}
P ⁵⁺ - Si	0.0	0.0	n.d.	n.d.
P ⁵⁺ - (PO) ³⁺	5.0	0.0	n.d.	n.d.
P ⁵⁺ - Al	-11.3	0.0	n.d.	n.d.
P ⁵⁺ - Fe ³⁺	0.0	0.0	n.d.	n.d.
P ⁵⁺ - Fe ²⁺	0.0	0.0	n.d.	n.d.
P ⁵⁺ - Mn	0.0	0.0	n.d.	n.d.
P ⁵⁺ - Ca	-17.59	0.0	n.d.	n.d.
Si - (PO) ³⁺	-9.2	-0.18	n.d.	n.d.
Si - Cr ³⁺	4.5	-0.33+1.0 X _{Si}	0.0	n.d.
Si - Al	2.0	-3.0	0.0	n.d.
Si - Fe ³⁺	1.0	1.6	0.0	n.d.
Si - Cr ²⁺	3.78	-1.02	0.0	n.d.
Si - Fe ²⁺	-1.5	2.1+1.0 X _{Si}	0.0	n.d.
Si - Mn	-4.5	-1.0+5.2 X _{Si}	-17.0	n.d.
Si - Mg	-8.0	1.2+3.0 X _{Si}	-10.8	n.d.
Si - Ca	-12.5	-4.5+7.5 X _{Si}	-0.2	0.0
(PO) ³⁺ - Al	-8.725	-15.05	n.d.	n.d.
(PO) ³⁺ - Fe ³⁺	0.0	5.0	n.d.	n.d.
(PO) ³⁺ - Fe ²⁺	19.0	12.0	n.d.	n.d.
(PO) ³⁺ - Mn	0.0	-19.2	n.d.	n.d.
(PO) ³⁺ - Ca	-21.2	-35.62	n.d.	n.d.
Cr ³⁺ - Al	1.92+0.76 X _{Cr}	-0.35+0.28 X _{Cr}	-4.0	n.d.
Cr ³⁺ - Fe ³⁺	3.0	0.0	0.0	n.d.
Cr ³⁺ - Cr ²⁺	3.42	-0.735	0.0	n.d.
Cr ³⁺ - Fe ²⁺	10.0	0.0	20.0	n.d.
Cr ³⁺ - Mn	-3.66	0.0	n.d.	n.d.
Cr ³⁺ - Mg	-0.82	-2.3	0.0	n.d.
Cr ³⁺ - Ca	-2.96	0.86	0.0	n.d.
Al - Fe ³⁺	0.0	0.0	0.0	n.d.
Al - Cr ²⁺	4.5	0.5	0.0	n.d.
Al - Fe ²⁺	-0.4	-2.3	-4.2	n.d.
Al - Mn	-1.2	-3.2	-11.625	n.d.
Al - Mg	-3.5	-7.0	3.0	n.d.
Al - Ca	-8.5+3.0 X _{Al}	-5.5-5.0 X _{Al}	14.45	0.0
Fe ³⁺ - Cr ²⁺	-1.0	0.0	0.0	n.d.
Fe ³⁺ - Fe ²⁺	-0.5	-0.5	-0.25	n.d.
Fe ³⁺ - Mn	-0.5	-0.5	0.0	n.d.
Fe ³⁺ - Mg	-3.7	-1.0	0.0	n.d.
Fe ³⁺ - Ca	-7.4	-2.0	1.2	0.0
Cr ²⁺ - Fe ²⁺	-1.6	0.0	0.0	n.d.
Cr ²⁺ - Mn	-1.66	7.12	n.d.	n.d.
Cr ²⁺ - Mg	2.0	-6.45	0.0	n.d.
Cr ²⁺ - Ca	10.0	-3.21	0.0	n.d.
Fe ²⁺ - Mn	-0.5	0.0	-10.1	n.d.
Fe ²⁺ - Mg	2.0	0.0	0.0	n.d.
Fe ²⁺ - Ca	-3.0	0.5	-0.6	0.0
Mn - Mg	0.0	0.0	0.0	n.d.
Mn - Ca	-0.5	-0.8	10.0	0.0
Mg - Ca	1.0	0.0	-0.35	0.0

Cation i	O - S exchange	
	W _i	E _i
Si	64.52	-0.2
Cr ³⁺	6.0	15.0
Al	32.0	7.5
Fe ³⁺	-1.5	-1.0
Cr ²⁺	30.0	0.0
Fe ²⁺	17.18	1.0
Mn	32.95	-8.0
Mg	31.45	0.0
Ca	14.2	0.0

Cation i	O - F exchange	
	W _i	E _i
Si	50.0	10.0
Al	50.0	6.0
Fe ²⁺	50.0	2.0
Mn	35.0	8.0
Mg	20.0	-4.5
Ca	0.0	-0.8

Cation i	S - F exchange	
	W _i	E _i
Al	18.0	-9.2
Mg	-11.45	0.0
Ca	-14.2	-2.31

Table 2: Values of the various model parameters which have been so far assessed (values expressed in kcal/mole)

Acknowledgements: Due to lack of space, it was not possible to give proper credit to the many authors whose results were used for the assessment. In addition, the authors would like to thank Prof. N. Sano, Tokyo University and Prof. I. Sommerville, University of Toronto, who provided some original unpublished data.

8. References.

[1] H. Gaye, J. Welfringer: 2nd Int. Symp. on "Metallurgical slags and fluxes", Warrendale, P.A. Met. Soc. of AIME, Ed. H.A. Fine and D. R. Gaskell, 1984, 357
 [2] H. Gaye, J. Lehmann, P.V. Riboud, J. Welfringer: Mém. Sci. Rev. Mét., 86 (1989), 237.
 [3] D.J. Sosinsky, I.D. Sommerville: Metall. Trans. B, 17 B (1986), 331.
 [4] J. Lehmann, H. Gaye, W. Yamada, T. Matsumiya: Proc. of the 6th IISC, 1990, Nagoya, ISIJ, 256.